IEEE Photonics Journal
An IEEE Photonics Society Publication

# Microwave Photonics Applications of Multicore Fibers

Volume 4, Number 3, June 2012

I. Gasulla
J. Capmany, Fellow, IEEE

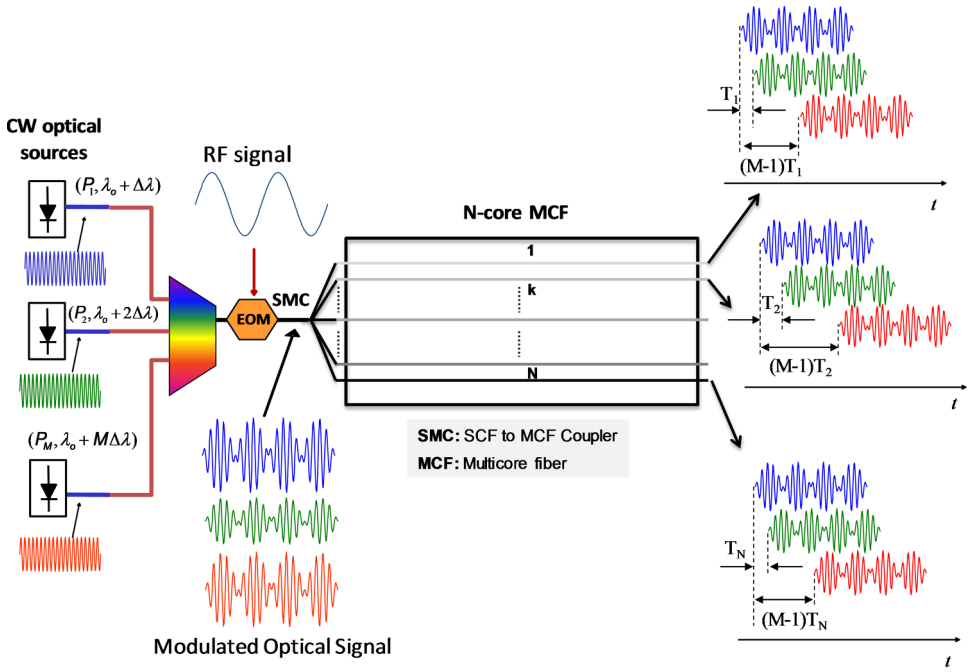


DOI: 10.1109/JPHOT.2012.2199101
1943-0655/$31.00 ©2012 IEEE

# Microwave Photonics Applications of Multicore Fibers

**I. Gasulla**[1] **and J. Capmany,**[2] ***Fellow, IEEE***

[1]Edward L. Ginzton Laboratory, Stanford University, Stanford, CA 94305 USA
[2]ITEAM Research Institute, Universidad Politecnica de Valencia, 46022 Valencia, Spain

*DOI: 10.1109/JPHOT.2012.2199101*
*1943-0655/$31.00 ©2012 IEEE*

Manuscript received March 28, 2012; revised May 2, 2012; accepted May 5, 2012. Date of publication May 11, 2012; date of current version May 25, 2012. Corresponding author: J. Capmany (e-mail: jcapmany@dcom.upv.es).

**Abstract:** This is the first time, to our knowledge, that the application of multicore fibers (MCFs) to the field of microwave photonics (MWP) has been proposed. The implementation of sampled optical delay lines for RF signals by means of heterogeneous MCFs is addressed as a generic building block and discussion is then centered on several selected applications including filtering, optical beamforming, and arbitrary waveform generation.

**Index Terms:** Microwave photonics (MWP), multicore fibers (MCFs), photonics generation, microwave photonic (MWP) filtering, optical beamforming.

## 1. Introduction

Multicore fibers (MCFs), invented three decades ago [1], have been recently the subject of considerable attention and research [2]–[7] as they enable the increase in the transmission capacity of optical fiber links by spatial division multiplexing (SDM). Reported research has mainly addressed digital transmission systems in several contexts as long haul transmission [2], combined polarization, wavelength and spatial multiplexing domains [3]–[6] and passive optical networks (PONs) [7]. The inherent parallelism offered by MCFs with potential low or negligible signal coupling between their inner cores makes them an ideal candidate for bandwidth extension in future telecommunication systems.

A vast majority of the research activity reported so far is based on the so-called homogeneous MCFs where identical cores are disposed in the fiber cross section following different profiles in order to either suppress or have a given control over mode coupling. Fundamental design parameters are the core *a* and cladding *b* diameters, and the core separation $\Lambda$, as shown in the upper part of Fig. 1.

Designs including 7 cores have been proposed and reported in the literature [7] and there is also a considerable activity being displayed by several groups in order to understand which is the best geometry and material composition to optimize their performance [8], [9].

There is an obvious interest in increasing the number of cores in MCFs and this requires the drastic reduction of mode coupling between the cores so they can be placed more tightly spaced within the cladding cross section. To this end, heterogeneous MCFs have been recently proposed [10]. In these, nonidentical cores, which are single mode in isolation of each other are arranged so, due to the absence of phase matching conditions, the crosstalk between any pair of cores is very small and thus can be more closely spaced. Although preliminary results have only been presented [11], MCFs with 19 and more cores are feasible and a broad field of design alternatives is expected

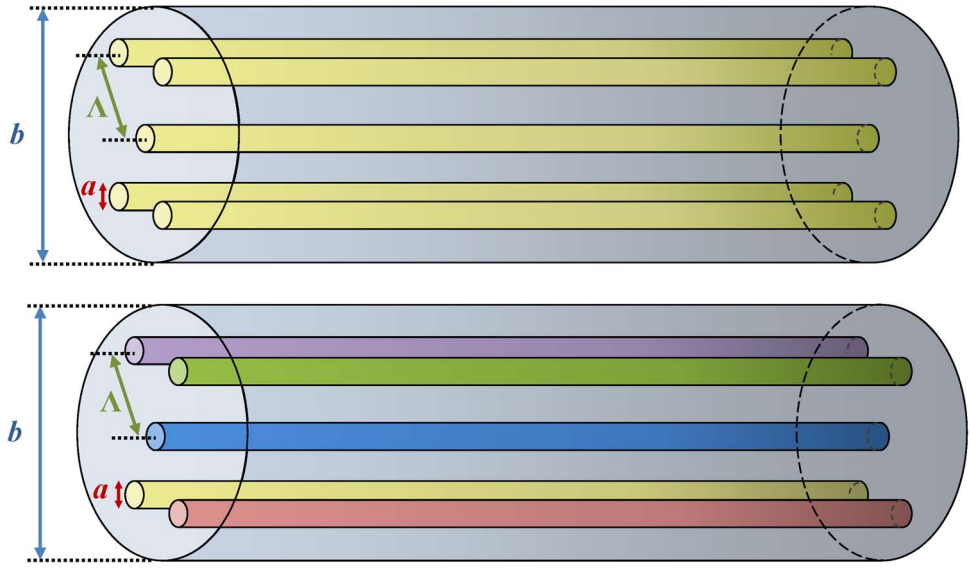


Fig. 1. Layouts for a homogeneous (upper) and heterogeneous (lower) multicore fiber including the relevant geometric design parameters.

to be proposed both in terms of geometric designs as well as of material compositions, which will require a thorough analysis using coupled-mode theory models for MCFs [12]. As mentioned before, most of the applications reported for MCFs have been restricted to the area of digital transmission. However, as it has happened with other photonic technologies, it is just a matter of time that novel application fields are suggested.

The aim of this paper is to propose the potential application of MCFs to the field of microwave photonics (MWP) [13], [14]. Their inherent parallelism makes them ideal candidates for the implementation of a sampled discrete true time delay line which is the basis of multiple functionalities in this field. We concentrate in particular on heterogeneous MCFs, where cores can be designed to have different dispersion profiles. The alternatives for the implementation of discrete time optical delay lines using single and multicarrier optical sources are discussed in Section 2. Specific applications to the field of MWP are presented in Section 3, where we have concentrated on three of the most important ones; signal filtering, optical beamforming and arbitrary waveform generation. Finally, in Section 4 we provide some conclusions as well as some future directions of research. Although heterogeneous MCFs with the desired characteristics are not yet available we aim to stimulate their middle term availability by proposing a novel field of application.

## 2. MCF-Based Sampled MWP Delay Lines

The basic building block is a sampled optical delay line based on a heterogeneous MCF. Throughout the paper we assume that each core acts as an independent single-mode waveguide transmitting a fundamental mode. In particular, the fundamental mode of core $j$ will have a propagation constant $\beta_j$, which we can approximate using a Taylor series around a central frequency of an optical source $\omega_o$

$$\beta_j(\omega) \approx \beta_j(\omega_o) + \left.\frac{d\beta_j(\omega)}{d\omega}\right|_{\omega=\omega_o}(\omega-\omega_o) + \frac{1}{2}\left.\frac{d\beta_j^2(\omega)}{d\omega^2}\right|_{\omega=\omega_o}(\omega-\omega_o)^2$$

$$= \beta_j^0 + \beta_j^1(\omega-\omega_o) + \frac{1}{2}\beta_j^2(\omega-\omega_o)^2. \quad (1)$$

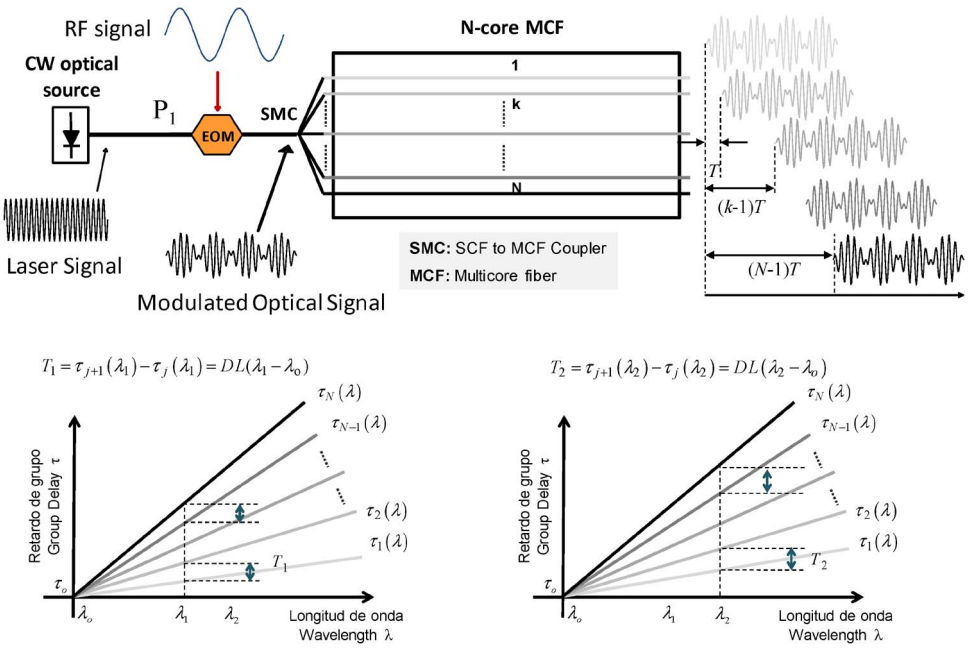


Fig. 2. Sampled delay line with spatial diversity output based on a heterogeneous MCF fed by a RF-modulated single optical carrier.

In a similar way the group delay of core $j$ at a given wavelength $\tau_j$ will be expressed as

$$\tau_j(\lambda) = L\frac{\lambda^2}{2\pi c}\frac{d\beta_j(\lambda)}{d\lambda} = L\left[\left.\frac{1}{v_{g,j}}\right|_{\lambda=\lambda_o} + D_j(\lambda-\lambda_o)\right] \tag{2}$$

where $L$ is the fiber length, $c$ the speed of light in vacuum, $v_{g,j} = 1/\beta_j^1$ represents the group velocity in core $j$ and $D_j$ is the first order chromatic dispersion parameter of core $j$ defined as

$$D_j = -\frac{2\pi c}{\lambda^2}\beta_j^2. \tag{3}$$

In this section we describe their operation and configuration principles by considering two possible implementation options. In first place we describe an implementation based on a heterogeneous MCF fed by a single input optical signal modulated by a RF subcarrier, where the different cores feature a different behavior in terms of chromatic dispersion. We then extend the concept to the case where the input is a RF modulated optical multicarrier signal fed to all the cores in the fiber.

### 2.1. Sampled Delay Line Fed by a Single Optical Carrier

Fig. 2 shows the basic configuration and illustrates the operation principle of the discrete optical delay line for RF signals based on the use of a single input optical carrier.

As shown in the upper part of Fig. 2, the sampled delay line is composed of a single CW laser source externally modulated (in amplitude or phase) by an input RF signal. The modulated input signal is evenly distributed among the $N$ cores of the heterogeneous MCF. The cores in the MCF have the same length $L$ but we shall assume that each one features a linear group delay characteristic as a function of the wavelength, although each one with a different slope (i-e a different first order chromatic dispersion parameter) as shown in the lower part of Fig. 2. Under this linear group delay dependence, the group delay provided by each core can be approximated by

$$\tau_j(\lambda) = \tau_o + jDL(\lambda-\lambda_o) \tag{4}$$

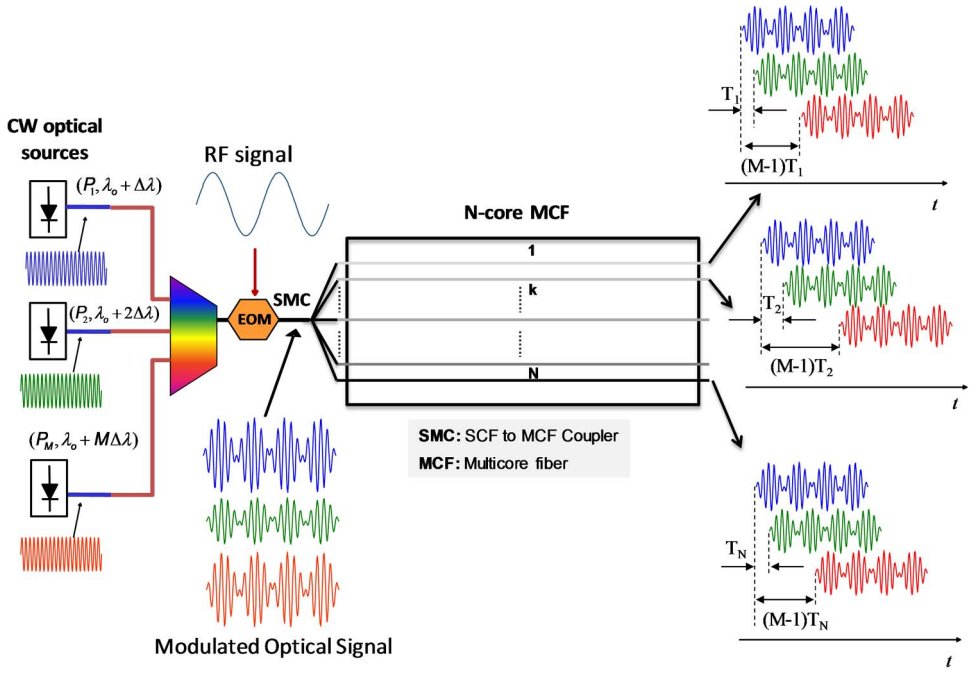


Fig. 3. Sampled delay line with spatial diversity output based on a heterogeneous MCF fed by a RF-modulated multiple optical carrier.

where $\lambda$ represent the optical wavelength, $j$ the core number, $D$ a common first order chromatic dispersion parameter and $\tau_o$ is a basic group delay common to all the cores for a given anchor or reference wavelength $\lambda_o$, $\tau_o = L/v_g$. The basic incremental delay at a wavelength $\lambda_k$ between the output signals from two cores featuring adjacent group delay characteristics is then given by

$$T_k = \tau_{j+1}(\lambda_k) - \tau_j(\lambda_k) = DL(\lambda_k - \lambda_o). \tag{5}$$

This incremental group delay value is fixed for a specific value of the wavelength. For example, the lower part of Fig. 2 shows the incremental group delay distribution when the operation wavelength is $\lambda_1$. In this case, the delay line produces $N$ replicas of the input RF-modulated optical signal delayed respectively by $0, T_1, 2T_1, \ldots, (N-1)T_1$. To change the value of the basic incremental delay one needs to tune the wavelength of the input CW source. For example, the lower part of Fig. 2 illustrates the change in the value of the basic incremental delay $T_1 \rightarrow T_2$, when the input source wavelength is tuned from $\lambda_1 \rightarrow \lambda_2$. At the MCF output $N$ equispaced samples (in time) of the input RF-modulated optical signal are obtained, where the basic intersample delay can be tuned. Each sample is obtained at the output of a different core so we shall use the term of *spatial diversity* to identify this configuration.

### 2.2. Sampled Delay Line Fed by a Multicarrier Source

An extension of the previous scheme where the input optical signal is of multicarrier nature (either by modelocking or by wavelength division multiplexing) is shown in Fig. 3. Referring to it the optical signal is composed by $M$ carriers where the central wavelengths are given by $\lambda_i = \lambda_o + i\Delta\lambda$, $i = 1, 2, \ldots, M$. This multicarrier signal is then RF modulated and injected to all the cores of the heterogeneous MCF. In this way, as it can be observed in Fig. 4, each multiplex experiences in each core $j$ a different basic incremental delay given by

$$T_j = \tau_j(\lambda_k) - \tau_j(\lambda_{k-1}) = jDL\Delta\lambda. \tag{6}$$

In other words, the output from each core corresponds to a sampled delay line providing $M$ delayed samples where each core features a different basic incremental delay.

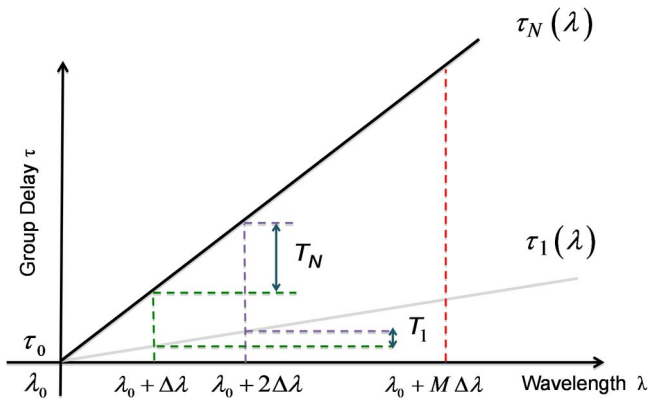


Fig. 4. Operation principle of the MWP optical delay line subject to multicarrier optical input RF-modulated signals. Illustration of the different incremental group delays obtained for each core.

This optical delay line actually provides a bidimesional delay configuration where the delay experienced by a RF signal sample carried by the wavelength $\lambda_i = \lambda_o + i\Delta\lambda$ and propagating through core $j$ is given by

$$\tau_{i,j} = \tau_o + ijDL\Delta\lambda. \tag{7}$$

This functionality can be exploited in two ways depending on whether the time or the wavelength domain is considered. In the first case, as it has been pointed before, the output of each core provides a different sampled delay line where the basic incremental delay is obtained by fixing the value of $j$ in (7) and then computing the difference between the delays experienced by wavelengths $i+1$ and $i$

$$T_j = jDL\Delta\lambda \tag{8}$$

In this way spatial diversity enables the implementation of $N$ independent delay lines, each one providing $M$ samples and a different basic intersample delay.

In the second case, which is illustrated in Fig. 5, the outputs from the $N$ cores can be combined and wavelength demultiplexed to obtain $M$ delay lines each one featuring $N$ samples where the basic incremental delay in each line is given by

$$T_i = iDL\Delta\lambda. \tag{9}$$

## 3. MWP Applications

We now consider the application of the sampled delay lines enabled by MCFs to a variety of applications in MWP. In particular, we concentrate on these which are generating more interest in the MWP research community in the last years: Filtering, Optical beamforming and arbitrary waveform generation.

### 3.1. Fixed and Tunable MWP Transversal Filtering

Both schemes presented in Section II can be employed for the implementation of discrete time MWP filters. The basic principles of these subsystems can be found in several papers in the literature [15], [16]. In essence, a discrete time MWP filter is described by means of an end to end transfer function [15]

$$H(\Omega) = \sum_{n=0}^{N-1} a_n e^{-j(n\Omega T+\phi_n)} \tag{10}$$

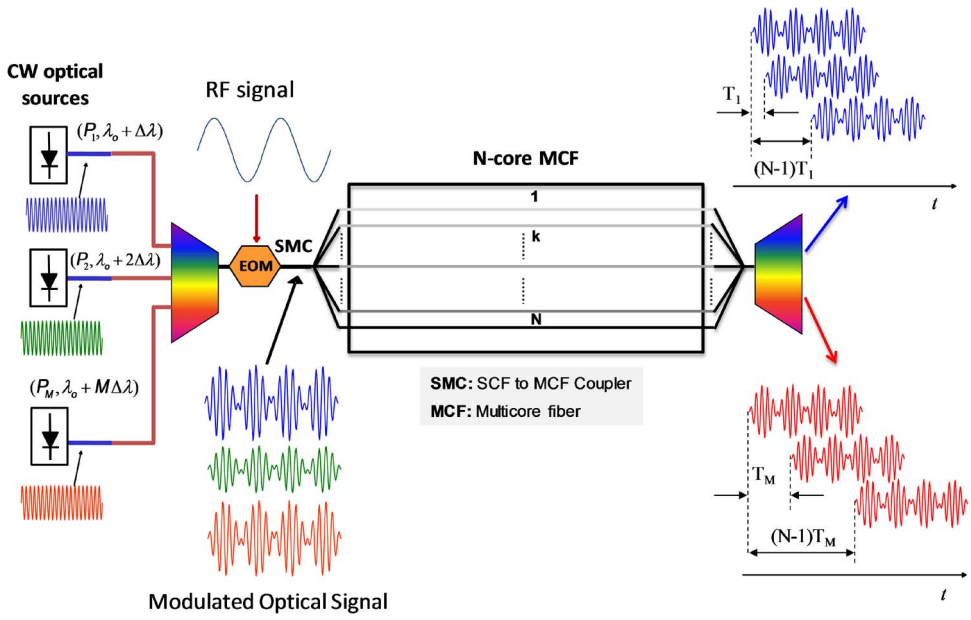


Fig. 5. Sampled delay line based on a heterogeneous MCF fed by a RF-modulated multiple optical carrier and WDM output demultiplexing.

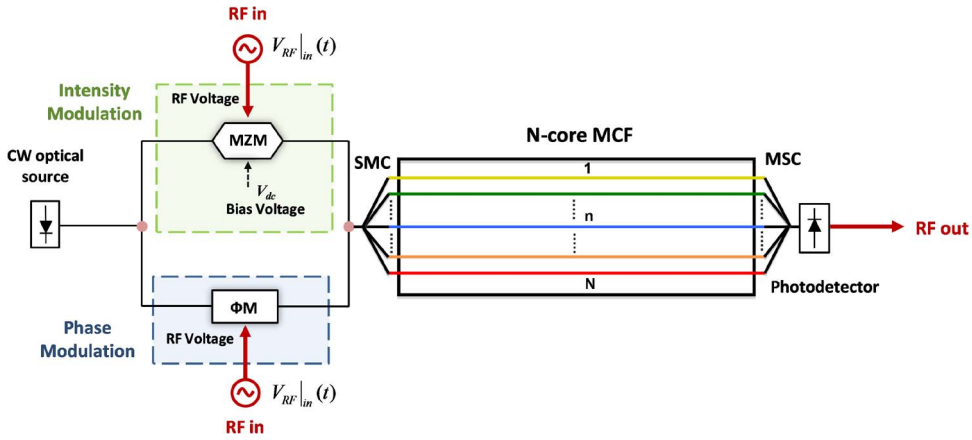


Fig. 6. Implementation of a discrete time MWP filter using a MCF-based sampled delay line fed by a single carrier optical source.

where $N$ represents the finite number of samples provided by the filter, $T$ the basic incremental delay between samples and $a_n$ and $\phi_n$ the amplitude and phase, respectively, of the $n$th sample.

Fig. 6 shows the proposal for the implementation of a discrete time MWP filter based on the single carrier sampled delay line. In essence the configuration is similar to that presented in Fig. 2 but in this case the output signals from each of the cores in the MCF must be combined and collectively detected by a single optical receiver. The incremental delay between samples is then given by (5) so tunable delays can be obtained by changing the wavelength of the input optical source resulting in the possibility of tuning the passbands provided by the filter. A fixed configuration is also possible if the wavelength of the optical carrier is kept unchanged.

The spatial diversity configurations of the sampled delay line implemented by means of a multicarrier optical source (shown in Figs. 3 and 5) can be exploited to provide parallel MWP filtering

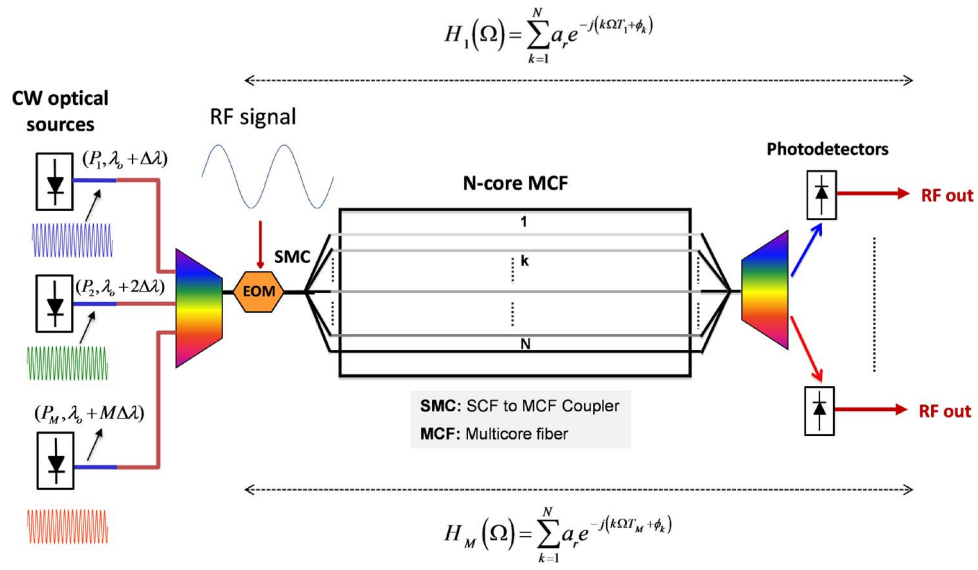


Fig. 7. Implementation of a discrete time MWP filter bank using a MCF-based sampled delay line fed by a multiple carrier optical source.

schemes. For instance Fig. 7 depicts an example of a bank of $M$ parallel discrete time filters $(H_1(\Omega), H_2(\Omega), \ldots, H_M(\Omega))$ implemented using the configuration of Fig. 5. Each filter has $N$ samples and a different basic intersample delay given by (9).

In a similar way, the configuration of Fig. 3 can be employed to implement a bank of $N$ parallel discrete time filters $(H_1(\Omega), H_2(\Omega), \ldots, H_N(\Omega))$, each filter having $M$ samples and a different basic intersample delay given by (7).

### 3.2. Optical Beamforming Networks for Phase Array Antennas

MWP subsystems and techniques can be advantageously employed in the implementation of the beamforming network that connects the input (output) to the antenna elements in an emitting (receiving) Phase Array Antenna system [14], [17]. To the usual advantages of low weight, low loss, and immunity to electromagnetic interference, MWP techniques bring other important added values such as fast angular scanning and radiation pattern shaping. Two features which are respectively very similar to the tuning and reconfiguration of MWP filters. In the case of a photonic beamforming network, the sampled true time delay implemented by means of a heterogeneous MCF fed by a single optical carrier can be also applied as shown, for instance, in Fig. 8 where the configuration is very similar to that proposed for discrete time filters in Fig. 6. The main difference here is that spatial diversity is kept as each of the $N$ cores injects its output signal to a different photodetector feeding a radiating element.

Referring to the layout displayed in Fig. 8, if $d_x$ represents the distance between adjacent radiating elements in the array and the beampointing direction $\theta$ is represented by $u = \sin(\theta)$, then the array factor is given by

$$AF(\theta) = \sum_{r=1}^{N} |a_r| e^{j\frac{r\Omega d_x}{c}(u-u_o)} \tag{11}$$

where $u_o = \sin(\theta_o)$, computed for $\theta_o$, the angle for which the array factor is maximum, is related to the incremental delay $T$ [given by (5)] by

$$u_o = \sin\theta_o = \frac{c}{d_x} T \tag{12}$$

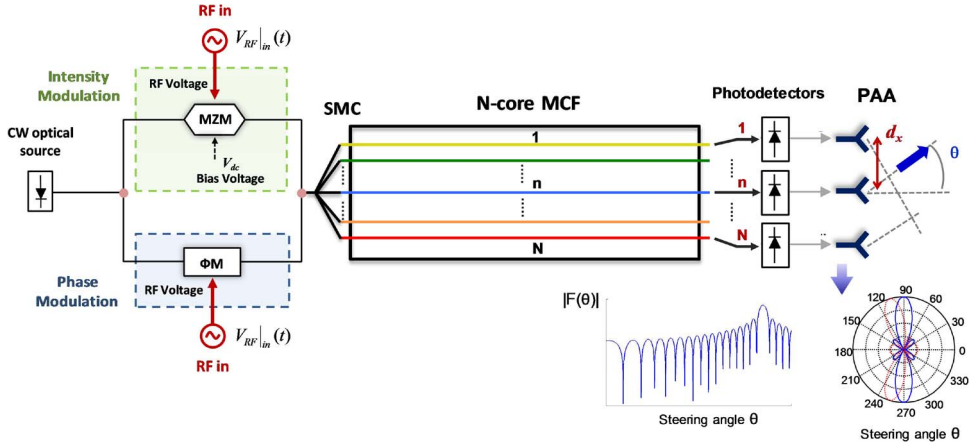


Fig. 8. Optical beamforming network implementation based on a heterogeneous MCF fed by a single carrier optical source.

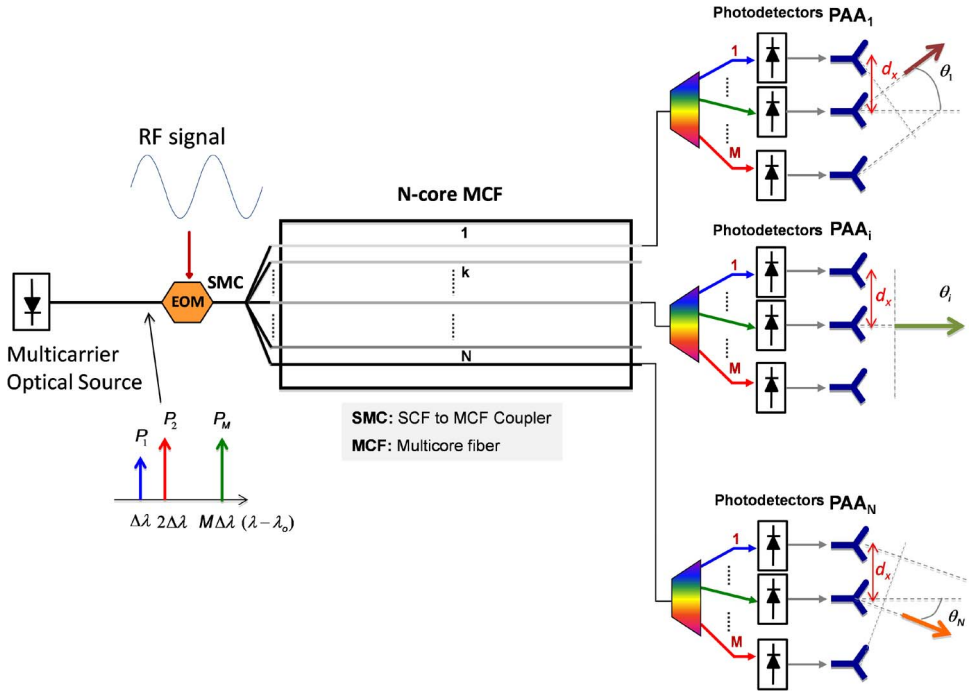


Fig. 9. Sectorized multibeam optical beamforming network implementation based on a heterogeneous MCF fed by a multicarrier optical source.

and $|a_r|$ are the power weighting coefficients which can be implemented by placing variable attenuators at the input of each photodetector to apodize the radiation pattern if required. As discussed in Section 2.1, the value of $T$ can be changed and thus the pointing direction of the radiation pattern scanned by tuning the wavelength of the CW input optical source. Furthermore, the bidimensional structure of the delays provided by the sampled delay line architectures based on multicarrier input sources and given by (7), is readily applicable to the implementation of 2-D and multibeam Phase Array Antenna configurations. For instance, Fig. 9 shows a configuration whereby sectorized multibeam pointing of the same input RF signal can be achieved in $N$ different pointing angles.

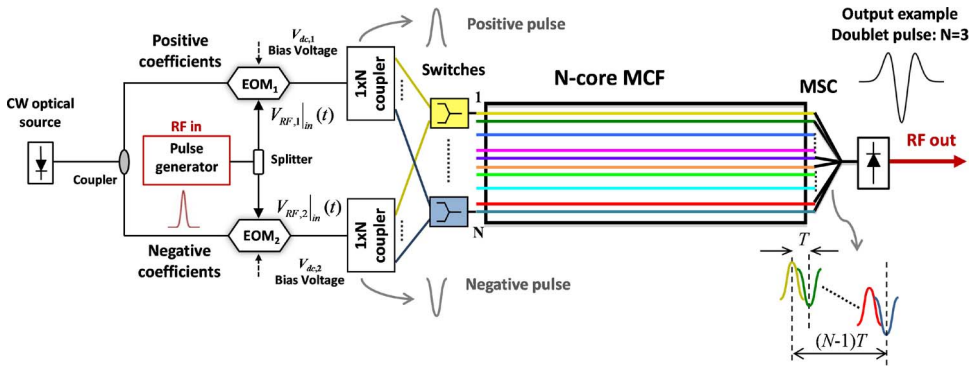


Fig. 10. Layout for the generation or arbitrary RF waveforms using a MCF and polarity inversion in Mach–Zehnder modulators.

### 3.3. Arbitrary Waveform Generation

As a final application example, we consider the use of the MCF-based sampled delay lines to the generation of arbitrary waveforms. Although the discussion presented here can be generalized to other signal formats we focus here on the generation of ultrawideband (UWB) using the discrete time MWP signal processing approach reported in [18]. UWB signal generation is based on the generation, delay and combination of pulses with different polarity. This means that a MCF based system designed for this purpose must incorporate the possibility of producing positive and negative taps. Two different configurations based on a MCF fed by a single carrier can be envisaged. The first one, shown in Fig. 10, employs two electrooptic modulators ($EOM_1$ y $EOM_2$) biased at their quadrature points, but on opposite slopes [15] $V_{dc,1}$ and $V_{dc,2}$, respectively. Both modulators are modulated by the same electrical input pulse. The modulated optical signal arising from $EOM_1$ is injected to a set of $N_1$ cores of the MCF and will provide $N_1$ weighted and delayed positive replicas of the input pulse. On the other hand, the modulated optical waveform arising from $EOM_2$ will be injected to a set of $N_2$ cores of the MCF providing $N_2$ weighted and delayed negative replicas of the input pulse. The final waveform synthesis is achieved by combining the outputs of the different cores in a single optical receiver. The flexibility of the generator in terms of sample delays follows the same roadmap as that required for tuning MWP filters, that is, by changing the value of the wavelength of the optical source the basic delay between pulse replicas can be modified. In terms of sample polarity full flexibility can be achieved by incorporating $1 \times N$ couplers, followed by $2 \times 1$ optical switches, so for a given sample its polarity can be selected by activating the switch in cross or bar state. Finally, the amplitude of each sample can be controlled by placing attenuators at the outputs of the $1 \times N$ couplers. As an example, Fig. 10 illustrates the case corresponding to the generation of a doublet pulse $N = 3(N_1 = 2, N_2 = 1)$ and a sample amplitude weight vector [0.5, $-1$, 0.5].

In the second approach a single Mach–Zehnder modulator is employed and sample polarity is implemented by means of a balanced differential detection preceded by $2 \times 1$ optical switching and $1 \times N$ combination stages as shown in Fig. 11.

The same principles described here for the generation of UWB pulses can be employed for other modulation formats such as pulse position modulation (PMM), biphase modulation (BPM), pulse amplitude modulation (PAM), orthogonal pulse modulation (OPM), etc.

## 4. Practical Considerations

The feasibility of the proposed concept relies on the possibility of implementing heterogeneous MCFs where the cores have the same length $L$ and a linear group delay characteristic as a function of the wavelength, although each one with a different slope, that is with a particular first order chromatic dispersion $D_j$, (3). In practice, since each core is independent, this can be achieved by acting over the material and/or waveguide dispersion of each one. Working over the material

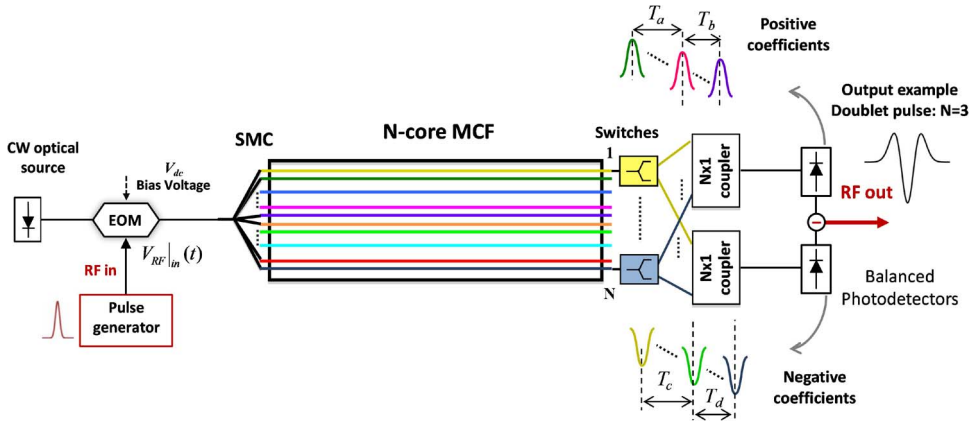


Fig. 11. Layout for the generation or arbitrary RF waveforms using a MCF and balanced differential detection.

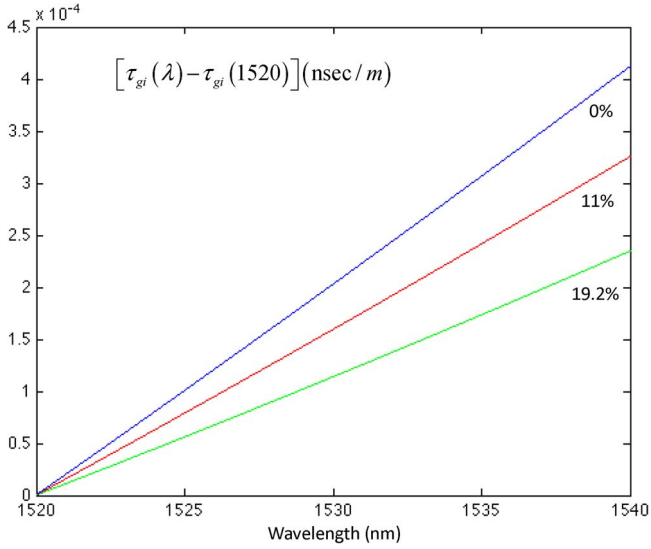


Fig. 12. Group delay versus wavelength for three Silica cores with different $GeO_2$ concentration.

dispersion will require the proper design of the refractive index profile of cores characterized by the same diameter *a*. For instance, we will assume a 3-core MCF, where each step-index core is characterized by a different core refractive index $n_{1,j}$, while sharing the same cladding refractive index $n_2$. Fig. 12 displays the group delay per unit length versus wavelength characteristics (2) of the 3 $SiO_2$ cores with different $GeO_2$ doping concentrations (fused Silica, 11%, and 19.2%) computed by means of the Sellmeier equation [19]. By compensating the basic delay for an anchor wavelength (in this case 1520 nm), three different $D_j$ values [20.5, 16, and 11.5 ps/(Km.nm)] are obtained.

Other techniques acting over the waveguide dispersion can be also employed in principle [20], in particular the change in the core diameter *a* of each independent core [21]. Further investigation is however required in the context of heterogeneous MCFs to clarify the most efficient process in terms of manufacturing process and design flexibility.

In the former 3-core example the common first order dispersion parameter, as defined in (4), is $D = 4.5$ ps/(Km.nm). By taking smaller $GeO_2$ concentration gaps it should be reasonable to expect the possibility of obtaining $D = 1$ ps/(Km.nm). For this value, Fig. 13 plots the expected radio

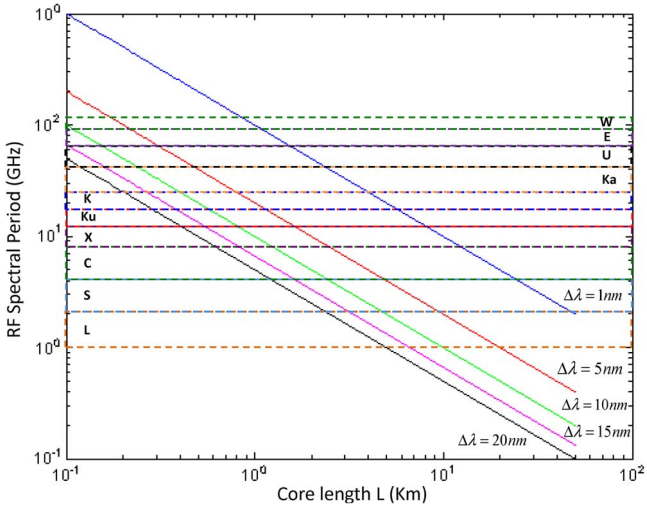


Fig. 13. RF spectral period versus the core length for a sampled delay line fed by a single optical carrier and characterized by a common first order dispersion parameter $D = 1$ ps/(Km.nm). The wavelength deviation of the optical source from 1520 nm $(\Delta\lambda)$ is taken as a parameter.

frequency spectral period [i.e., $1/T_k$ as given by (5)] in GHz provided by a sampled optical delay line fed by a single optical carrier as a function of the core length $L$ in Km. The wavelength separation from 1520 nm is taken as a parameter. The area enclosed by the broken rectangle corresponds to the range of RF spectral periods which are useful in the field of MWP, that is ranging from 1 to 100 GHz (L, S, C, X, Ku, K, Ka, U, E, W bands). As it can be observed, a maximum core length of around 1 Km is required for a full coverage of the complete spectral range. This requirement is however relaxed if smaller ranges are targeted. For example, covering the RF and microwave spectrum, up to the Ku band (12–18 GHz) fixes the maximum core length to about 7 Km, while for the distribution of UWB signals (up to 10.6 GHz), the maximum core length would be in the range of about 10 Km. These values illustrate the potential application of the proposed sampled delay lines to a variety of MWP applications.

## 5. Summary and Conclusion

This is the first time, to our knowledge, that the application of MCFs to the field of MWP has been proposed. The implementation of sampled optical delay lines for RF signal processing by means of heterogeneous MCFs has been first addressed as a generic building block and discussion on potential applicability has been then centered on several selected microwave applications including filtering, optical beamforming and arbitrary waveform generation. Practical issues regarding the alternatives to implement group delay characteristics with different linear slopes in each core have been discussed and the feasibility for obtaining delays within the ranges required by the spectra of RF, microwave and millimeter wave applications have been considered. The application of the proposed sampled delay line to other fields such as radio over fiber transmission and analog to digital conversion is quite straightforward following the basic principles that have been presented. As a final remark, we would like to point out that despite the fact that heterogeneous MCFs are not yet available, we envisage that these and other application areas, in particular digital transmission systems, will fuel their industrial development. Once available, the experimental verification of the applications presented here will be a valuable direction of research.

## References

[1] S. Inao, T. Sato, S. Sentsui, T. Kuroha, and Y. Nishimura, "Multicore optical fiber," presented at the Optical Fiber Communication OSA Tech. Dig., Tucson, AZ, 1979, Paper WB1.

[2] T. Hayashi, T. Toshiki, S. Osamu, S. Takashi, and S. Eisuke, "Ultra-low-crosstalk multicore fiber feasible to ultra-long haul transmission," presented at the OFC/NFOEC, Los Angeles, CA, 2011, Paper PDPC.
[3] J. Sakaguchi, Y. Awaji, N. Wada, A. Kanno, T. Kawanishi, T. Hayashi, T. Taru, T. Kobayashi, and M. Watanabe, "109-Tb/s (7 $\times$ 97 $\times$ 172-Gb/s) SDM/WDM/PDM) QPSK transmission through 16.8-km homogeneous multicore fiber," presented at the OFC/NFOEC, Los Angeles, CA, 2011, Paper PDPB6.
[4] B. Zhu, T. F. Taunay, M. Fishteyn, X. Liu, S. Chandrasekhar, M. F. Yan, J. M. Fini, E. M. Monberg, F. V. Dimarcello, K. Abedin, P. W. Wisk, D. W. Peckham, and P. Dziedzic, "Space-, wavelength-, polarization-division multiplexed transmission of 56-Tb/s over a 76.8-km seven-core fiber," presented at the OFC/NFOEC, Los Angeles, CA, 2011, Paper PDPB7.
[5] J. Sakaguchi, Y. Awaji, N. Wada, T. Hayashi, T. Nagashima, T. Kobayashi, and M. Watanabe, "Propagation characteristics of seven-core fiber for spatial and wavelength division multiplexed 10-Gbit/s channels," presented at the OFC/NFOEC, Los Angeles, CA, 2011, Paper OWJ2.
[6] B. Zhu, T. F. Taunay, M. Fishteyn, X. Liu, S. Chandrasekhar, M. F. Yan, J. M. Fini, E. M. Monberg, and F. V. Dimarcello, "112-Tb/s space-division multiplexed DWDM transmission with 14-b/s/Hz aggregate spectral efficiency over a 76.8-km seven-core fiber," *Opt. Exp.*, vol. 19, no. 17, pp. 16 665–16 671, Aug. 2011.
[7] B. Zhu, T. F. Taunay, M. F. Yan, J. M. Fini, M. Fishteyn, E. M. Monberg, and F. V. Dimarcello, "Seven-core multicore fiber transmissions for passive optical network," *Opt. Exp.*, vol. 18, no. 11, pp. 11 117–11 122, May 2010.
[8] K. Imamura, Y. Tsuchida, K. Mukasa, R. Sugizaki, K. Saitoh, and M. Koshiba, "Investigation on multi-core fibers with large Aeff and low micro bending loss," *Opt. Exp.*, vol. 19, no. 11, pp. 10 595–10 603, May 2011.
[9] K. Takenaga, Y. Arakawa, S. Tanigawa, N. Guan, S. Matsuo, K. Saitoh, and M. Koshiba, "Reduction of crosstalk by trench-assisted multi-core fiber," presented at the OFC/NFOEC, Los Angeles, CA, 2010, Paper OWk7.
[10] M. Koshiba, K. Saitoh, and Y. Kokubun, "Heterogeneous multi-core fibers: Proposal and design principle," *IEICE Electron. Exp.*, vol. 6, no. 2, pp. 98–103, 2009.
[11] Y. Kokubun and T. Watanabe, "Dense heterogeneous uncoupled multi-core fiber using 9 types of cores with double cladding structure," in *Proc. 17th IEEE MOC*, 2011, pp. 1–2.
[12] M. Koshiba, K. Saitoh, K. Takenaga, and S. Matsuo, "Multi-core fiber design and analysis: coupled-mode theory and coupled-power theory," *Opt. Exp.*, vol. 19, no. 26, pp. B102–B111, Dec. 2011.
[13] J. Capmany and D. Novak, "Microwave photonics combines two worlds," *Nat. Photon.*, vol. 1, no. 6, pp. 319–330, Jun. 2007.
[14] J. Yao, "Microwave Photonics," *J. Lightw. Technol.*, vol. 27, no. 3, pp. 314–335, Feb. 2009.
[15] J. Capmany, B. Ortega, D. Pastor, and S. Sales, "Discrete-time optical processing of microwave signals," *J. Lightw. Technol.*, vol. 23, no. 2, pp. 702–723, Feb. 2005.
[16] R. A. Minasian, "Photonic signal processing of microwave signals," *IEEE Trans. Microw. Theory Tech.*, vol. 54, no. 2, pp. 832–846, Feb. 2006.
[17] R. J. Mailloux, *Phased Array Antenna Handbook,* 2nd ed. Dedham, MA: Artech House, 2000.
[18] J. P. Yao, F. Zeng, and Q. Wang, "Photonic generation of ultrawideband signals," *J. Lightw. Technol.*, vol. 25, no. 11, pp. 3219–3235, Nov. 2007.
[19] D. Marcuse, "Pulse distortion in singlemode fibers," *Appl. Opt.*, vol. 19, no. 10, pp. 1653–1660, May 1980.
[20] A. F. Mendez and T. F. Morse, *Specialty Optical Fibers Handbook*. New York: Academic, 2007.
[21] T. Hayashi, T. Sasaki, and E. Sasaoka, "Microbending-induced crosstalk increase in heterogeneous multi-core fiber," in *Proc. 37th ECOC*, 2011, pp. 1–3.